Springer Series in

Optical Sciences

Lasers and Applications

Editors:
W.O.N. Guimaraes C.-T. Lin A. Mooradian

Springer-Verlag
Berlin Heidelberg New York Tokyo

Lasers and Applications

Proceedings of the Sergio Porto Memorial Symposium
Rio de Janeiro, Brasil, June 29 - July 3, 1980

Editors:
W.O.N. Guimaraes, C.-T. Lin, and A. Mooradian

With 200 Figures

Springer-Verlag
Berlin Heidelberg New York Tokyo

Professor WLADIMIR O.N. GUIMARAES
Instituto de Fisica, Unicamp
13.100 Campinas Sp, Brasil

Professor CHHUI-TSU LIN
Instituto de Quimica, Unicamp
13.100 Campinas Sp, Brasil

Dr. ARAM MOORADIAN
Massachusetts Institute of Technology,
Lincoln Laboratory
Lexington, MA 02173, USA

Editorial Board

Second Printing 1985

ISBN 3-540-10647-2 Springer-Verlag Berlin Heidelberg New York Tokyo
ISBN 0-387-10647-2 Springer-Verlag New York Heidelberg Berlin Tokyo

Offset printing: Beltz Offsetdruck, Hemsbach/Bergstr. Bookbinding: J. Schäffer oHG, Grünstadt.
2153/3130-543210

Preface

The International Conference on Lasers and Applications was held in Rio de Janeiro, Brazil from 29 June to 3 July 1980. This conference was held to commemorate the memory of Professor Sergio Porto who died suddenly about one year earlier while attending a laser conference in the Soviet Union. The subject matter covered the active areas of laser devices, photochemistry, nonlinear optics, high-resolution spectroscopy, photokinetics, photobiology, photomedicine, optical communication, optical bistability, and Raman spectroscopy.

The conference was attended by over 150 people including scientists from Japan, France, England, West Germany, Norway, Italy, Brazil, Chile, Argentina, India, Canada, and the United States. A memorial session attended by members of the Porto family and ranking Brazilian government dignitaries preceded the start of the conference.

The location of the conference in Rio de Janeiro, Brazil, was chosen because it was in the homeland of Sergio Porto and provided an opportunity for his friends, colleagues, and countrymen to pay homage to him. The setting on Copacabana Beach afforded access to the lovely beaches, restaurants, and nightlife of one of the most beautiful and exciting cities of the world. There were tours of the city together with a banquet that featured a performance by one of the best Samba Schools in Rio.

Financial support from many sponsors in Brazil and the United States is gratefully acknowledged in making this working conference a fitting tribute to the memory of Professor S.P.S. Porto.

January, 1981

W.O.N. Guimaraes
C.T. Lin
A. Mooradian

Contents

Part III. *Laser Photochemistry*

Part IV. *New Laser Devices and Applications*

Part V. *Laser Biology and Medicine*

Part VI. *Picosecond Bistability*

Part I

Raman Spectroscopy

Surface Brillouin Scattering

R. Loudon

Physics Department, Essex University, Colchester CO4 3SQ, UK

1. Introduction

During the past 20 years, since the invention of the laser, light scattering has become an increasingly powerful means of measuring the spectra of systems in thermal equilibrium. Sergio Porto played a leading role in the development of techniques to take maximum advantage of the properties of laser light in its application to light scattering, and he and his collaborators made many of the first observations of the spectra of excitations which thereby became accessible to this kind of measurement. The power spectra of the thermal fluctuations of almost all dynamic variables in solids and liquids can be studied by light scattering over part of the range of frequency and wavevector.

Most light scattering work of the past two decades has been concerned with excitations in bulk materials but there has been a parallel interest in the spectra of surface excitations. For example, in the case of light scattering by thermally-excited surface waves on a liquid, where experimental observations date back to 1913 [1], the first measurements of the ripplon frequency spectra were made in 1967 and 1968 [2,3], followed by more detailed investigations [4]. The measurements are made on flat surfaces; we consider only this case.

It is possible to distinguish two effects that arise in the presence of a surface. Firstly, the fluctuations associated with the bulk modes of excitation are modified close to the surface because of the boundary conditions imposed on the dynamic variable concerned. Secondly, there are usually new modes of excitation whose fluctuations have significant amplitude only at or very close to the surface. For a liquid, the longitudinal acoustic waves are bulk modes while the ripplons are surface modes.

2. Surface Fluctuations

The total surface fluctuation in a dynamical variable is calculated, as in the bulk case [5], from the energy of a static displacement of the variable concerned. Fig. 1 shows the co-ordinates and geometry to be used throughout, with the z=0 plane as the surface of the undisturbed medium, and the excitation wavevector taken as (Q, 0, q). Consider a static ripple on a liquid, with vertical displacement

$$u^z(0) = u_0 \cos Q x \qquad u_0 Q << 1. \qquad (1)$$

To lowest order in u_0, the increase in area of a large section of the surface of area A is

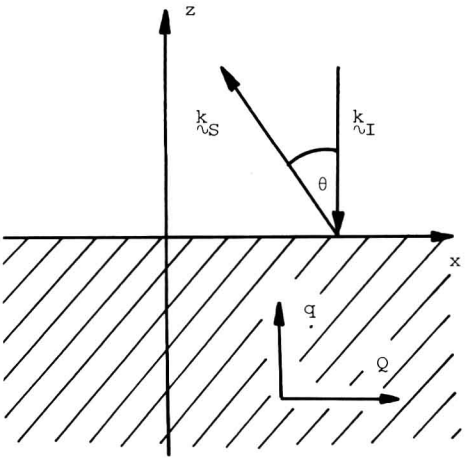

Fig.1. Surface light-scattering geometry

$$\Delta A = \frac{1}{4} u_0^2 Q^2 A \ . \tag{2}$$

The energy of the ripple is given by a sum of the gravitational and surface-tension contributions,

$$\Delta E = \frac{1}{4} u_0^2 A(\rho g + \alpha Q^2) \ , \tag{3}$$

where α is the surface tension and ρ is the density. The classical thermal excitation factor $\exp(-\Delta E/k_B T)$ then leads to a mean-square displacement

$$\langle u^z(0)^2 \rangle_Q = \frac{1}{2} \langle u_0^2 \rangle = k_B T/A(\rho g + \alpha Q^2) \ . \tag{4}$$

This is the integrated surface displacement spectrum for ripples with a given direction of surface wavevector Q.

The total mean-square surface displacement obtained by summation over all wavevectors is

$$\begin{aligned} \langle u^z(0)^2 \rangle &= (A/4\pi^2) \int_0^{Q_m} \langle u^z(0)^2 \rangle_Q \, 2\pi \, Q \, d \, Q \\ &\approx (k_B T/4\pi \alpha) \log(\alpha \, Q_m^2/g\rho) \ . \end{aligned} \tag{5}$$

If the maximum wavevector is taken to be that for which the viscous damping rate equals the ripple frequency, then numerical values for mercury at room temperature give

$$Q_m \approx 3 \times 10^9 \ m^{-1} \qquad \langle u^z(0)^2 \rangle^{\frac{1}{2}} \approx 1.4 \times 10^{-10} \ m \ , \tag{6}$$

a root-mean-square displacement of about 3 Bohr radii. The wavevectors Q accessible to light-scattering spectroscopy lie typically in the range

$$10^5 \ m^{-1} < Q < 10^7 \ m^{-1} \ , \tag{7}$$

where the surface-tension energy greatly exceeds the gravitational, and (4) can be written

$$\langle u^z(0)^2 \rangle_Q = k_B T/A \propto Q^2 \ . \tag{8}$$

The results for other kinds of surface fluctuation are obtained in a similar manner. Thus for surface ripples on an isotropic solid, where the restoring force results from the elastic stiffness expressed in terms of the Lamé parameters λ and μ, the mean-square surface displacement is

$$\langle u^z(0)^2 \rangle_Q = k_B T(\lambda + 2\mu)/2A\mu(\lambda + \mu)Q \ . \tag{9}$$

The root-mean-square displacement obtained by summation over all wavevectors gives

$$\langle u^z(0)^2 \rangle^{\frac{1}{2}} \approx 2.3 \times 10^{-11} \text{ m} \tag{10}$$

for aluminium, equal to about one half the Bohr radius. Note that for a liquid where the shear stiffness μ is zero, the fluctuations become unrestrained unless surface tension is included.

Electromagnetic fluctuations can be treated similarly. The perpendicular component of the electric field at the surface of a dielectric with static relative permittivity κ_o has a mean-square fluctuation

$$\langle E^z(0)^2 \rangle_Q = k_B T \, Q/\varepsilon_o \, A \, \kappa_o(1 + \kappa_o) \ . \tag{11}$$

The fluctuations may be associated with surface plasmons or polaritons. Finally, for a ferromagnet with applied field H_o and spontaneous magnetization M_o parallel to the y axis, the magnetization perpendicular to the surface has a mean-square fluctuation

$$\langle M^z(0)^2 \rangle_Q = k_B T \, \gamma \, M_o/\mu_o \, A \, D^{\frac{1}{2}}(\gamma H_o + D \, Q^2)^{\frac{1}{2}} \ , \tag{12}$$

where γ is the gyromagnetic ratio and D is the exchange stiffness.

The varying dependence of the strength of the fluctuations on Q has important consequences for light-scattering experiments. For ripples on liquids, where the surface tension energy proportional to Q^2 is confined to the surface itself, the same factor Q^2 appears in the denominator of (8). For ripples on solids the elastic energy in a layer of given z-co-ordinate is also proportional to Q^2. However, the distortion now penetrates some distance into the bulk material with a spatial dependence that includes a term of the form

$$u^z(z) = u_o \exp(Qz) \cos Qx \ . \tag{13}$$

The penetration depth is thus proportional to $1/Q$, and the volume-integrated elastic energy is proportional to Q, giving the factor Q in the denominator of (9). Similar qualitative remarks apply to the other examples. We note that the spatial dependence (13) occurs in the static limit for any excitation whose total wavevector is proportional to a positive power of the frequency.

The common thermal factor $k_B T$ in the fluctuations is a consequence of the classical statistics, and the results are incorrect when the main contributions occur at angular frequencies comparable to or larger than $k_B T/\hbar$. The main contributions to the electric-field fluctuations associated with surface polaritons usually occur at angular frequencies of order 10^{13} Hz, when (11) is invalid. Such frequencies correspond to Raman scattering rather than

Brillouin scattering and we consider this case no further. For comparison, with a surface wavevector Q of order 10^7 m^{-1}, the main acoustic-wave contributions to the surface ripple spectra occur at angular frequencies of order 10^{10} Hz for both solids and liquids, and the ferromagnetic spin wave frequencies are also in this region. The liquid ripplon frequencies are of order 10^8 Hz. The classical statistics are valid in these cases.

3. Kinematics and Techniques

For the scattering of light by an excitation of surface wavevector Q and frequency ω, the incident and scattered optical wavevectors and frequencies are related by

$$k_I^x = k_S^x \pm Q \tag{14}$$

$$\omega_I = \omega_S \pm \omega, \tag{15}$$

where the upper (lower) signs refer to the Stokes (anti-Stokes) components of the scattered light.

Suppose for example that the incident light beam is normal to the sample surface and that scattered light is collected at angle θ to the normal, as shown in Fig. 1. Then (14) and (15) give

$$\omega/\omega_I = \pm 1 - (cQ/\omega_I) \operatorname{cosec} \theta. \tag{16}$$

Fig. 2 shows the scans across the ωQ plane for various scattering angles. The excitation wavevectors that contribute to the anti-Stokes spectrum are slightly larger than those that contribute to the Stokes spectrum for a given θ, but the differences are negligible in a typical Brillouin experi-

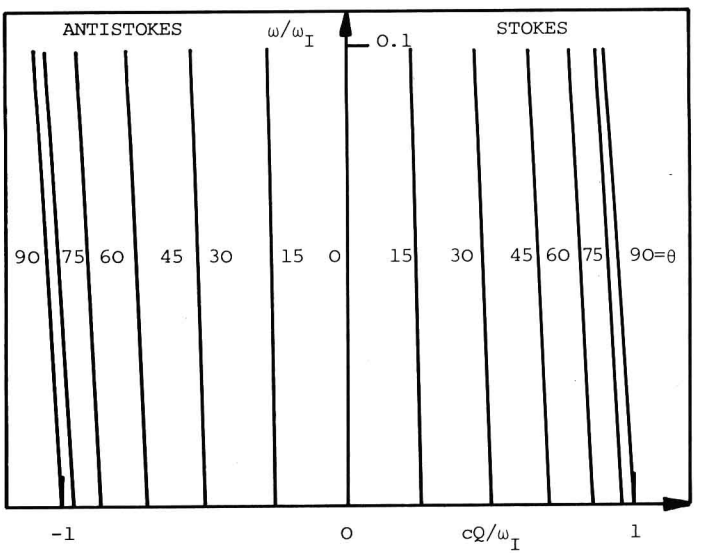

Fig.2. Experimental scans for various scattering angles

ment where ω/ω_I is of order 10^{-4} or less. The most important feature is the change in sign of the wavevector of the excitation with which the light interacts between the two sides of the spectrum. Thus although the wavevector transfer Q is the same for the entire spectrum, the Stokes side corresponds to creation of a quantum of excitation of wavevector Q and the anti-Stokes side to destruction of a quantum with wavevector -Q. This can lead to assymetry in the measured spectra around $\omega=0$ in systems that are not invariant under time reversal, for example ordered magnetic materials or media with an externally generated flow of acoustic waves.

Two main experimental techniques are used to measure surface Brillouin spectra. For ripplons, with frequency

$$\omega_R = (\alpha Q^3/\rho)^{\frac{1}{2}} \tag{17}$$

and a scattered intensity obtained from (8) proportional to $1/Q^2$ there are advantages in achieving small Q, of order 10^5 m^{-1} in practice, by scattering close to the direction of specular reflection of the incident light. Then ω_R is typically of order 10^5 Hz and the scattered light is resolved by optical heterodyne spectroscopy. For the acoustic wave and magnetic spectra, where the dependences of intensity on Q given by (9) and (12) are less rapid and the frequencies are generally higher, the spectra are best measured by Fabry-Perot interferometry. Brillouin scattering measurements in this regime have been dominated by the work of John Sandercock using progressively refined multipass interferometers.

Theoretical analysis of the measurements requires the calculation of fluctuation spectra, and not merely their integrated values discussed in §2. The required spectra are readily obtained by linear response theory [6] in terms of the susceptibility of the excitation variable to a suitable applied force of frequency ω. The imaginary part of the susceptibility (or linear response function or Green function) determines the frequency spectrum of the excitation via the fluctuation-dissipation theorem.

4. Liquid Fluctuation Spectra

The spectrum of the mean-square surface displacements on a viscous liquid calculated by linear response theory [7] is

$$\left\langle u^z(0)^2 \right\rangle_{Q,\omega} = \frac{2k_BT}{\pi A\omega} \operatorname{Im} \frac{i\, q_L (q_T^2 + Q^2)^2}{(q_T^2 - Q^2)^2 \rho\omega^2 + q_L Q^2 \{4\rho\omega^2 q_T + i\alpha(q_T^2 + Q^2)^2\}} \tag{18}$$

where

$$q_L = \{(\omega/V_L)^2 - Q^2\}^{\frac{1}{2}} \tag{19}$$

$$q_T = \{(i\rho\omega/\eta) - Q^2\}^{\frac{1}{2}} \tag{20}$$

are the components of the longitudinal and transverse wavevectors perpendicular to the surface, V_L is the longitudinal acoustic velocity, and η is the shear viscosity. Fig. 3 shows the calculated spectrum for mercury for $Q = 10^7$ m^{-1}. With increasing frequency, the first spectral contribution comes from the surface modes, centred on the frequency (17) and with a modest width $4\eta Q^2/\rho$. The second much broader contribution, commencing at a

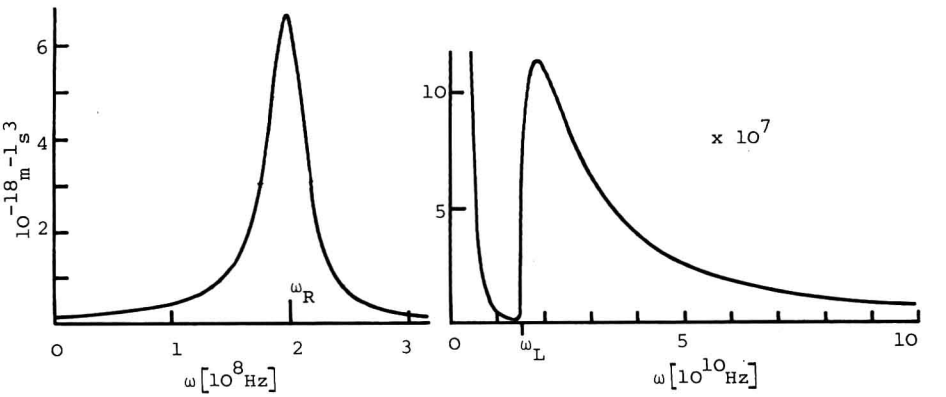

Fig.3. Calculated surface-ripple spectrum of mercury

frequency

$$\omega_L = V_L Q \ , \tag{21}$$

comes from the bulk modes, the longitudinal acoustic waves. The bulk modes give a broad continuous distribution because for a given Q in (19) the wavevector component q_l perpendicular to the surface can take all values from 0 to ∞, producing a range of frequencies ω. The intrinsic damping caused by the viscosity has a negligible broadening effect on the continuum.

The ripplon part of the spectrum measured experimentally [8,9] is much broader than expected from the ordinary value of the viscosity, but the measured acoustic wave part [10] is in close agreement with the calculated spectrum. More recent work has studied spectra of fluids covered by monolayers [11] and there remain various problems in the spectra of more complex fluid surfaces.

5. Solid Fluctuation Spectra

The spectrum of the mean-square surface displacements on an isotropic solid has a calculated form almost identical to (18). However, the presence of shear restoring forces in the solid causes changes in the interpretation of some of the symbols. There are now propagating transverse acoustic waves with velocity V_T given by

$$\rho V_T^2 = \mu \ , \tag{22}$$

and their wavevector z component is

$$q_T = \{(\omega/V_T)^2 - Q^2\}^{\frac{1}{2}} \ , \tag{23}$$

replacing (20). The longitudinal velocity is expressed in terms of the Lame parameters by

$$\rho V_L^2 = \lambda + 2\mu \ . \tag{24}$$

The surface displacements are restored by the elastic stiffness forces, much stronger than the surface tension in a liquid, and α can be set equal to zero in (18).

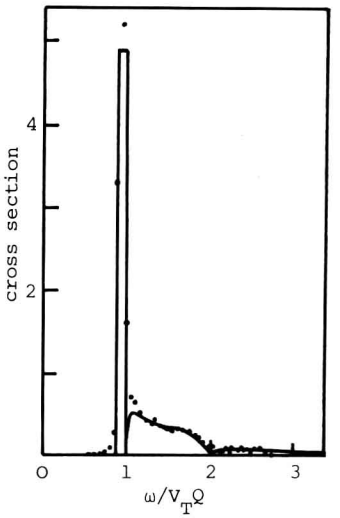

Fig.4. Calculated spectrum and measured points for surface ripples on aluminium (from [15])

Figure 4 shows the measured [12] and calculated [13-16] surface fluctuation spectra of polycrystalline aluminium. Because there is now only one kind of force in the system, all of the spectrum occurs in the same frequency region. The surface mode is the Rayleigh acoustic wave; the theory does not include the anharmonic forces that generate its damping, and the rectangle in Fig. 4 shows the integrated area of this contribution. The continua to higher frequencies come from the bulk transverse and longitudinal acoustic waves.

In the spectra described above, where the media are metals, the coupling of incident and scattered light occurs via the surface distortion. The cross section is derived by a generalization of ordinary reflectivity theory, where the flat surface is perturbed by a travelling ripple [15,17,18]. In less opaque materials, where the incident light penetrates further, the ripple mechanism is augmented by the elasto-optic mechanism responsible for the normal bulk scattering, where the coupling of incident and scattered light occurs by way of the acoustic modulation of the relative permittivity. The elasto-optic mechanism contributes for excitations where the influence of the surface extends some distance into the bulk material. The surface Brillouin spectra of several solids show the effects of simultaneous scattering by the two mechanisms [19-22].

Other kinds of surface excitation produce no mechanical distortion of the surface and their light-scattering spectra result solely from the elasto-optic mechanism. For a solid film mounted on a solid substrate, there are various modes that have an oscillatory spatial dependence in the film but decay exponentially with distance into the substrate. With the co-ordinates of Fig. 1, there are Sezawa waves polarized in the zx plane that produce a surface rippling and have been observed experimentally [23,24], and there are Love waves polarized in the y direction that scatter only by the elasto-optic mechanism [25] and have not so far been observed. This collection of waves originally discovered in seismic studies is completed by the Stoneley waves that propagate along the interface between two media and scatter by both mechanisms [26].

Magnetic excitations do not of course produce any significant surface ripple, and their light scattering occurs entirely by the magneto-optical modulation of the relative permittivity. The cross section is thus determined not merely by the fluctuations in magnetization at the z=0 surface but also by their spatial dependence. The bulk and surface mode fluctuations have different spatial dependences and their relative contributions to the scattering are sensitive to the optical penetration depth. Surface effects should occur for all kinds of ordered magnetic material but most work to date is concerned with ferromagnets.

The surface mode frequency of a ferromagnet in the magnetostatic limit is

$$\omega_M = \gamma(H_o + \frac{1}{2} M_o) \ , \tag{25}$$

and the associated fluctuations have a mean-square magnetization component [27]

$$\left\langle M^z(z)^2 \right\rangle_{Q,\omega} = (k_B T \gamma M_o Q/\mu_o A \omega_M) \exp(2Qz) \delta(\omega \pm \omega_M) \ . \tag{26}$$

The most intriguing aspect of the magnetic surface spectra is the lack of symmetry between the Stokes and anti-Stokes sides. Thus in (26), the positive sign is to be taken in the delta function when the wavevector transfer of magnitude Q is directed parallel to the x-axis, but the negative sign is to be taken when the wavevector transfer is directed antiparallel to the x axis. With a given experimental geometry the surface mode therefore contributes a peak either to the Stokes or to the anti-Stokes side of the spectrum, but not to both sides.

Figure 5 shows the calculated spectrum [28,29] for Fe when the wavevector transfer is positive. Note that the bulk modes contribute more conventionally with symmetrically placed continua. The calculated magnetic Brillouin spectra give good interpretations of the measurements [30,31]. There is potential for further studies of bulk and surface magnetic modes in ordered samples by Brillouin spectroscopy, particularly to determine the role of surface perturbations [32].

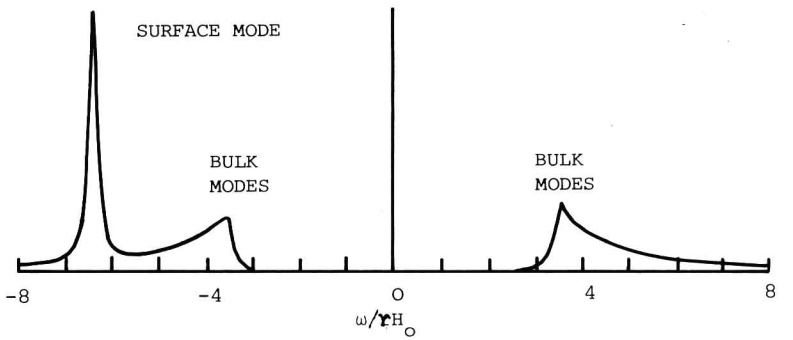

Fig.5. Calculated surface magnetic spectrum of iron (from [22])